Screened Coulomb interaction in the maximally localized Wannier basis

Takashi Miyake and F. Aryasetiawan
Research Institute for Computational Sciences, AIST, Tsukuba 305-8568, Japan
and Japan Science and Technology Agency, CREST, 4-1-8, Honcho, Kawaguchi-shi, Saitama 332-0012, Japan
(Received 22 October 2007; published 27 February 2008)

We discuss a maximally localized Wannier function approach for constructing lattice models from first-principles electronic structure calculations, where the effective Coulomb interactions are calculated in the constrained random-phase approximation. The method is applied to the 3*d* transition metals and a perovskite ($SrVO_3$). We also optimize the Wannier functions by unitary transformation so that *U* is maximized. Such Wannier functions unexpectedly turned out to be very close to the maximally localized ones.

DOI: 10.1103/PhysRevB.77.085122 PACS number(s): 71.15.−m, 71.28.+d, 71.10.Fd

I. INTRODUCTION

In a class of materials often referred to as correlated materials, the electronic structure is characterized by a set of partially filled narrow bands across the Fermi level. Seen from the atomic site, one has a set of partially filled shell of localized orbitals typically of 3*d* or 4*f* character. Many of the electronic properties of the material are determined by the correlations among the localized electrons living in the partially filled band or shell. It is, therefore, physically well motivated to map the original complicated many-electron problem to a model consisting of the localized orbitals and a few additional orbitals. By eliminating the high-energy states ("downfolding"), the long-range bare Coulomb interaction is screened to a short-range interaction at low energy. Since the screened interaction is short range, only on-site interaction or the Hubbard *U* is often taken into consideration in the model. This is the physical idea behind the well-known Hubbard model or Andersen impurity model. One would then wish to have a set of well localized orbitals or Wannier orbitals that span the same Hilbert space as that of the states that form the narrow bands. In this way the Hubbard *U* will have small off-site matrix elements, which may be neglected. Practical procedures to construct the models starting from first-principles calculations have been a subject of interest for a long time.[1–4]

In this work, we focus on Wannier orbitals using the method developed by Souza, Marzari, and Vanderbilt[5,6] based on the minimization of the quadratic extent of the orbitals. An alternative, equally promising approach is to use the Wannier orbitals of Andersen and co-workers.[7] While the former is a "postprocessing" method, i.e., the Wannier orbitals are constructed after generating the Bloch wave functions, the latter may be termed "preprocessing" method because the Wannier orbitals are constructed before diagonalization of the Hamiltonian that yields the band structure. In this sense, the latter scheme may be more advantageous than the former. On the other hand, the former is more general because it does not depend on any particular band-structure method. Comparison between the two Wannier functions for some selected materials can be found in Ref. 8.

Apart from the use of Wannier orbitals in constructing lattice models, there are many other applications. In particular, a close connection with Berry's phase[5,9] has stimulated intensive works recently.[10–13] Related work can be found not only in condensed matter physics but also in chemistry, where the concept of localized molecular orbitals is very useful for understanding chemical bonding as well as for visualization. The idea of constructing localized molecular orbitals goes back to the early 1960s by the maximization of the Coulomb energy of the molecular orbitals[14] or the minimization of the quadratic extent of the molecular orbitals.[15] The general problem of transforming a set of Bloch states to a set of well localized orbitals is, therefore, one of important methodological problems in condensed matter physics and chemistry.

Another important issue in the downfolding procedure is how to determine effective interaction parameters. A widely used method is constrained local density approximation (cLDA),[1,2,16] and a recently proposed scheme based on the maximally localized Wannier function[17] may be useful for applications to complicated structures. On the other hand, cLDA is known to yield unreasonably large values of *U* in some cases (e.g., late transition metals). This arises from technical difficulty in including part of the self-screening processes between localized electrons, leading in some cases to a larger value of *U*.[18] Another method for estimating effective interaction is the random-phase approximation (RPA). We can find early trials along this line in Refs. 19 and 20. Later on the constrained RPA (cRPA) scheme was invented.[3] The cRPA method has several advantages over currently available methods. It allows for a precise elimination of screening channels, which are to be included in a model Hamiltonian, without modifying the one-particle dispersion of the model. In addition, the effective screened interaction as a function of $\mathbf{r}$ and $\mathbf{r}'$ can be calculated independent of the basis functions. We will use this method in the present work. We can also find other proposals in literature such as a hybrid method between cLDA and cRPA,[21] and linear response approach.[22]

Our long-term goal is to construct a first-principles scheme for calculating the electronic structure of correlated materials. As is well known, the local density approximation[23] (LDA) in density functional theory[24] (DFT) often has difficulties when applied to such systems. Attempts to improve the LDA have resulted, among others, in the LDA+*U*,[16,25,26] the LDA+DMFT (dynamical mean-field theory[27,28]),[29] and, more recently, in the newly developed GW+DMFT method.[30,31] In Ref. 31, it is shown how the

Hubbard U for real materials can be determined self-consistently within the scheme. In these methods, it is crucial to have well localized orbitals representing the Hilbert space of the partially filled correlated bands since the screened Coulomb interaction U is usually assumed to be purely on-site. This is especially the case in the DMFT method, where the lattice problem is mapped to an impurity problem.[32]

The purpose of the present work is to demonstrate the usefulness of the Wannier orbitals and the feasibility of performing many-body calculations with a unified Wannier basis, independent of the starting band structure. To this end, we have calculated the Hubbard U within the cRPA scheme using the maximally localized Wannier basis and compared the results with independent calculations[3,18] in the linear muffin-tin orbital (LMTO) basis.[33] The reasonably good agreement between the two sets of results gives us confidence as to the usefulness of the scheme.

As mentioned earlier, it is highly desirable to construct a set of Wannier orbitals that minimize the off-site Coulomb interaction or equivalently maximizes the on-site U. We follow the method of Edmiston and Ruedenberg,[14] which was proposed for molecules, and develop a practical procedure to maximize the U parameter for periodic crystals through unitary transformation in real space. Application to transition metals shows that the effect of maximization is small if we start the optimization from the maximally localized Wannier functions.

II. METHOD

The Wannier function with band index n at cell $\mathbf{R}$ is defined by

$$|\varphi_{n\mathbf{R}}\rangle = \frac{V}{(2\pi)^3}\int e^{-i\mathbf{k}\cdot\mathbf{R}}|\psi_{n\mathbf{k}}^{(\mathrm{w})}\rangle d^3k, \tag{1}$$

where $|\psi_{n\mathbf{k}}^{(\mathrm{w})}\rangle$ is the associated Bloch function, which can be expanded as a linear combination of the eigenfunctions of a mean-field Hamiltonian as

$$|\psi_{n\mathbf{k}}^{(\mathrm{w})}\rangle = \sum_m \mathcal{U}_{mn}(\mathbf{k})|\psi_{m\mathbf{k}}\rangle. \tag{2}$$

In practical implementations, Kohn-Sham wave functions may be used for $|\psi_{m\mathbf{k}}\rangle$. In the maximally localized Wannier function scheme,[5,6] the coefficients $\mathcal{U}_{mn}(\mathbf{k})$'s are determined such that the quadratic extent of wave functions

$$\Omega = \sum_n (\langle\varphi_{n0}|r^2|\varphi_{n0}\rangle - |\langle\varphi_{n0}|\mathbf{r}|\varphi_{n0}\rangle|^2) \tag{3}$$

is minimized. For this purpose, we introduce an energy window and optimize $\mathcal{U}_{mn}(\mathbf{k})$ by limiting m to the states inside the window. The parameters for this window ("window 1") are listed in Table I. The Wannier function is more localized as the energy window is larger, since optimization is done in a wider Hilbert space. We found, however, that the (screened) Coulomb interaction is not sensitive to the choice of the energy window unless the window is too wide. In more detail, the optimization is done in two steps. We first choose the Hilbert space out of states inside window 1, then symmetrize the Wannier functions via Löwdin's procedure and minimize their spread through unitary transformation. The symmetrized Wannier functions without the minimization in the second step are recently used for the analysis of correlated materials.[34]

TABLE I. Energy window 1 that limits states to be included in constructing Wannier functions, and window 2 to specify localized orbitals $\{\psi_d\}$ for cRPA. The "2nd band" for window 2 means the second lowest one in the bands with strong $4s$ and $3d$ character. Energies are measured from the Fermi level.

	Window 1	Window 2
Sc	[−3.0 eV,5.0 eV]	[2nd band, 4.05 eV]
Ti	[−4.0 eV,5.0 eV]	[2nd band, 3.85 eV]
V	[−4.0 eV,5.0 eV]	[2nd band, 4.15 eV]
Cr	[−5.0 eV,4.0 eV]	[2nd band, 2.85 eV]
Mn	[−5.0 eV,4.0 eV]	[2nd band, 1.50 eV]
Fe	[−5.0 eV,4.0 eV]	[2nd band, 1.20 eV]
Co	[−5.0 eV,3.0 eV]	[2nd band, 0.55 eV]
Ni	[−7.0 eV,3.0 eV]	[2nd band, 0.25 eV]
$SrVO_3$	[−10.0 eV,5.0 eV]	3 t_{2g} states

The idea of cRPA is to define an effective interaction W_r by excluding screening processes that are included in an effective low-energy model, with W_r as the effective interaction (Hubbard U). To this end we divide the Hilbert space into two parts: localized states that form the projected bands $\{\psi_d\}$ and the rest $\{\psi_r\}$. The polarizability P is then divided into two as $P=P_d+P_r$, where P_d includes transitions between $\{\psi_d\}$ only and P_r is the rest of the polarization. The effective interaction in the reduced space W_r is defined so that $W_r[1-P_dW_r]^{-1}$ yields the RPA fully screened interaction $W=v[1-Pv]^{-1}$, where v is the bare Coulomb interaction. It can be shown that such W_r is given by

$$W_r(\omega) = v[1 - P_r(\omega)v]^{-1}, \tag{4}$$

where spatial coordinates are omitted for simplicity.[3] This W_r, after multiplying some localized functions and integrating over space, can be interpreted as the frequency-dependent Hubbard U. We refer the static value of $W_r(0)$ as the Hubbard U used in model Hamiltonians.

In the following sections, we compute matrix elements of W_r in the Wannier basis. The calculation starts with a conventional LDA electronic structure obtained by the full-potential LMTO method.[35] The polarizability is computed using Kohn-Sham eigenfunctions and eigenvalues. It can be computed efficiently for an arbitrary number of frequencies at essentially the cost of just one frequency.[36] Other technical details are found elsewhere.[37–41] We use an $8\times8\times8$ k mesh for transition metals and a $4\times4\times4$ k mesh for $SrVO_3$ for the Brillouin zone integration. Optimization of Wannier functions is done following the procedure in Refs. 5 and 6.

III. CONSTRAINED RANDOM PHASE APPROXIMATION WITH THE MAXIMALLY LOCALIZED WANNIER FUNCTION

Let us start with paramagnetic nickel as an example. We first construct five Wannier orbitals having strong $3d$ charac-

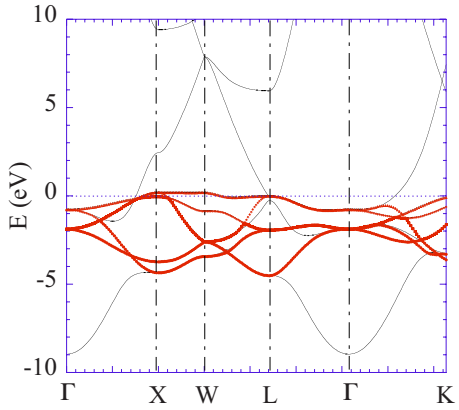

FIG. 1. (Color online) Band structure of paramagnetic nickel in LDA (solid thin lines) and projected bands (dotted thick lines).

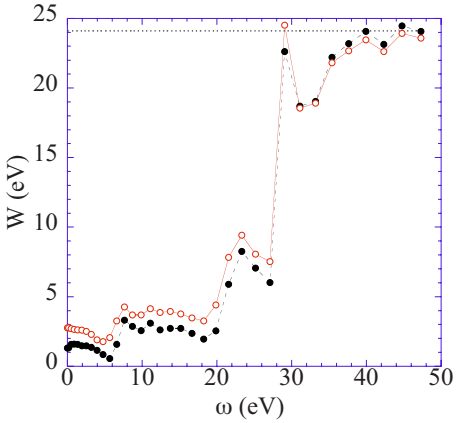

FIG. 2. (Color online) On-site screened Coulomb interaction of paramagnetic nickel in the maximally localized Wannier basis as a function of frequency: fully screened interaction (closed circles), result from cRPA (open circles), and bare Coulomb interaction (dotted line).

ter. Once $\mathcal{U}_{mn}(\mathbf{k})$ is determined on a k mesh, maximally localized Wannier functions are obtained by Fourier transform, from which the Hamiltonian $H_{mn}(\mathbf{R})=\langle\varphi_{m\mathbf{0}}|H|\varphi_{n\mathbf{R}}\rangle$ is reduced as well. By Fourier transforming $H_{mn}(\mathbf{R})$ back to k space and diagonalizing it,[6] we can project out narrow bands (Fig. 1).

The next step is to compute the screened Coulomb interaction $W_r(\mathbf{r},\mathbf{r}';\omega)$ in cRPA and take the matrix elements in the maximally localized Wannier basis:

$$W_r(n_1,n_2,n_3,n_4;\mathbf{R};\omega) \equiv \int\int \varphi^*_{n_1\mathbf{0}}(\mathbf{r})\varphi_{n_2\mathbf{0}}(\mathbf{r})W_r(\mathbf{r},\mathbf{r}';\omega) \times \varphi^*_{n_3\mathbf{R}}(\mathbf{r}')\varphi_{n_4\mathbf{R}}(\mathbf{r}')d^3r d^3r'. \quad (5)$$

At this point, it is worth pointing out that the effective screened interaction $W_r(\mathbf{r},\mathbf{r}';\omega)$ calculated using the cRPA method is completely independent of the choice of basis functions. The matrix elements are, of course, dependent on the choice of the orbitals $\varphi_{n\mathbf{0}}(\mathbf{r})$. The on-site diagonal elements, $W_r(n,n,n,n,\mathbf{R}=\mathbf{0};\omega)$ $(n=1,\ldots,5)$, are split by crystal field effect; however, the splitting is negligibly small. Figure 2 shows the average of the five diagonal elements where fully screened Coulomb interaction is also shown for comparison. W_r is close to the bare Coulomb value (dot-dashed line) at high energy, since screening effect is minor. As the frequency decreases down to around 30 eV, the screening becomes effective and W_r decreases rapidly. At lower energy, W_r is weakly energy dependent again and reaches 2.8 eV at $\omega=0$. These features are the same as the previous calculations,[3,18] though the values are slightly smaller in the present result. The difference may be ascribed to the difference in spacial extent of the orbitals $\varphi_{n\mathbf{0}}(\mathbf{r})$. In the previous calculations, the effective screened interaction $W_r(\mathbf{r},\mathbf{r}';\omega)$ is calculated within the LMTO-ASA (where ASA denotes atomic sphere approximation) scheme and the orbitals $\varphi_{n\mathbf{0}}(\mathbf{r})$ are taken to be the truncated partial waves, i.e., the heads of the LMTO or the solutions of the Schrödinger equation inside the atomic sphere, rather than the LMTO basis. They are normalized and completely confined to the atomic spheres. In the present calculations, $W_r(\mathbf{r},\mathbf{r}';\omega)$ is calculated using the full-potential LMTO (FP-LMTO) scheme, but the orbitals $\varphi_{n\mathbf{0}}$ are the maximally localized Wannier functions, which have tail extending outside the central cell. These orbitals are, thus, more delocalized and consequently, the matrix elements of W_r are smaller. The difference in $W_r(\mathbf{r},\mathbf{r}';\omega)$ arising from the difference between LMTO-ASA and FP-LMTO is probably less significant.

The above information, projected band structure and on-site values of W_r, are key ingredients for constructing effective models. However, it is not sensible to construct a Hubbard model by simply adding the former as the kinetic term and the static value of the latter as the interaction term. In fact, excitation spectra for that Hamiltonian do not reproduce the solution of the original Hamiltonian. This is because (i) the kinetic term is renormalized during the downfolding process, and (ii) W_r is energy dependent and long ranged. However, there is an approximate way to construct a Hubbard Hamiltonian with a static interaction.[3]

Figure 3(a) shows the diagonal element of the on-site W_r in the static limit (U) for a series of transition metals. Comparing the results with those obtained from previous calculations presented in Fig. 3(b), the trend is the same: As the atomic number increases, the U increases in the early transition metals, while it decreases in late transition metals. We also computed U in $SrVO_3$ (Table II). In this system, there are three t_{2g} states near the Fermi level and they are isolated from other bands. Thus, there is no ambiguity in dividing the space into $\{\psi_d\}$ and $\{\psi_r\}$. The value of U is computed to be 3.0 eV, which is again smaller than the previously calculated value of 3.5 eV. We emphasize again that in the previous calculations, the effective screened interaction W_r is calculated within the LMTO-ASA scheme and the choice of the orbitals in calculating the matrix elements of W_r are truncated partial waves, which are confined within the atomic sphere and, thus, more localized compared with the Wannier orbitals used in the present calculations, leading to a larger value of U. The U value obtained for $SrVO_3$ should be similar for $CaVO_3$, $LaTiO_3$, and $YTiO_3$ perovskites.

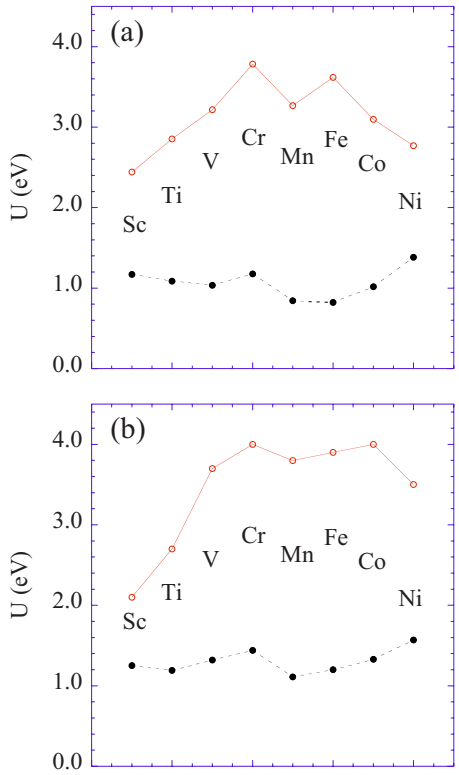

FIG. 3. (Color online) On-site screened Coulomb interaction U for transition metals from cRPA (open circles) and fully screened U from RPA (closed circles). Results when the matrix elements of $U = W_r(\omega=0)$ are taken (a) in the maximally localized Wannier function basis and (b) in the truncated partial waves or the heads of the LMTO-ASA basis.

The off-diagonal (exchange) elements are also important quantities. In Fig. 4(a), $\langle W_r(n,m,m,n,\mathbf{R}=\mathbf{0};\omega)\rangle_{n\neq m}$ in Ni is shown as a function of frequency, where the average is taken over n and m. In contrast to the Coulomb term, the exchange term is weakly energy dependent and does not show significant change at around 30 eV. We may understand this behavior as follows. $\int d^3r' W_r(\mathbf{r},\mathbf{r}';\omega)\varphi^*_{n_3\mathbf{R}}(\mathbf{r}')\varphi_{n_4\mathbf{R}}(\mathbf{r}')$ is a screened potential of a charge density $\rho(\mathbf{r}') = \varphi^*_{n_3\mathbf{R}}(\mathbf{r}')\varphi_{n_4\mathbf{R}}(\mathbf{r}')$. In accordance with known observation, the potential arising from an exchange charge density ($n_3 \neq n_4$) is not well screened because it has no monopole (zero spherical average) in contrast to the case of $n_3=n_4$. At the onset of the plasmon excitation at around 30 eV, a perturbing charge is highly screened and the screening is electron-gas-like, which is highly effective for a monopole. At lower energy (5–6 eV), however, atomiclike screening in the form of $3d$-$3d$ transitions as well as $3d$-$4p$ takes place, which is relatively effective in screening a multipole charge distribution, resulting in a significant decrease of J. As can be seen in the case of Fe and Ni, J is reduced considerably when $3d$-$3d$ screening arising from P_d is included, whereas in Cu, where there are essentially no $3d$-$3d$ transitions, since the $3d$ band is fully occupied, the main screening channels come from $3d$-$4p$ transitions and J varies less strongly compared to those of Ni and Fe for the fully screened case. Figure 5 shows the static value of the exchange term, J. In agreement with common assumption, we find that J does not depend on the element significantly and its value is around 0.6–0.7 eV. However, this value is reduced by approximately 20% compared with the atomic value, which is about 0.8 eV.

TABLE II. On-site Coulomb (U), exchange (J), and off-site Coulomb (U') energies in $SrVO_3$ obtained by cRPA.

U	3.0 eV
U'	0.45 eV
J	0.43 eV

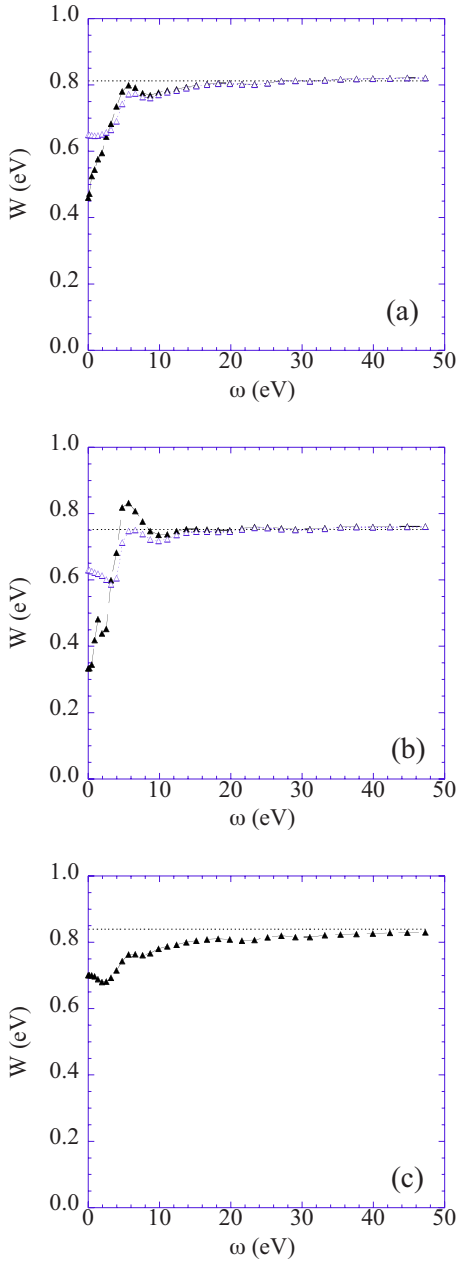

FIG. 4. (Color online) On-site exchange interaction from fully screened interaction (closed triangles), cRPA (open triangles), and from bare interaction (dotted line) in (a) Ni, (b) Fe, and (c) Cu.

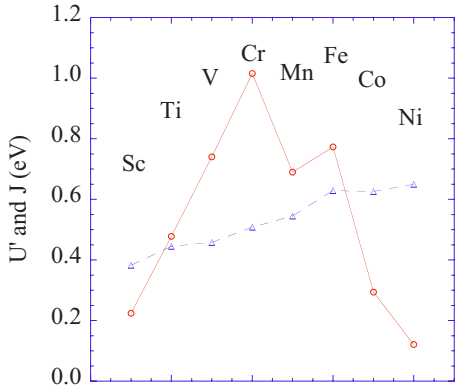

FIG. 5. (Color online) On-site screened exchange interaction J (triangles) and off-site screened Coulomb interaction U' (open circles).

Another important information is the nonlocality of the interactions. The bare Coulomb interaction v as a function of $R=|\mathbf{R}|$ is long ranged [Fig. 6(a)], and v between the nearest neighbor cells is about $1/4$ of the on-site value. On the other hand, the screened interaction shows much faster damping and the value at the nearest neighbor (U') is 0.1 eV, which is much smaller than the on-site value of $U=2.7$ eV. The values of U' for other transition metals are shown by open circles in Fig. 5.

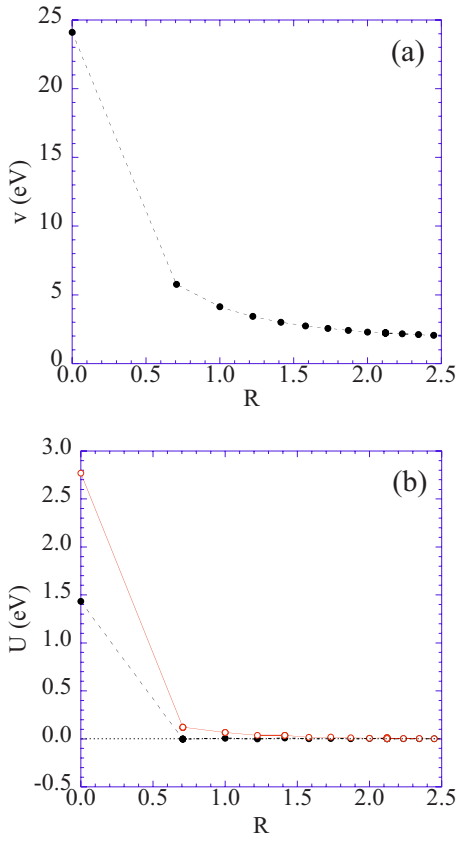

FIG. 6. (Color online) Diagonal elements of Coulomb interaction of Ni as a function of $R=|\mathbf{R}|$ (in units of lattice constant). (a) Bare Coulomb interaction and (b) screened Coulomb interactions in cRPA (open circles) and in RPA (closed circles).

The approximately parabolic variation on both U and U' across the series may be qualitatively understood in terms of $3d$ band filling. The largest polarization inside the $3d$ band (P_d) corresponds roughly to half-filling. Since this is eliminated when calculating U and U', they peak around the middle of the series. This is in contrast to the fully screened interaction W, which is almost a constant across the series. As discussed in Ref. 3, since the screening is metallic, it does not depend much on the element: there are always enough electrons to screen a perturbing charge. Moreover, since the screened interaction is rather localized, it is not sensitive to the extent of the orbitals used in taking the matrix elements in Eq. (5).

The U' is larger in some elements. For example, U' of Cr is as large as 1.0 eV, which would not be negligible. In such cases, one would wish to reconstruct the Wannier function so that off-site interaction is as small as possible. This possibility is discussed in the next section, where a procedure to maximize the on-site U is derived and applied.

IV. MAXIMIZING THE ON-SITE U PARAMETER

A. Formulation

We follow closely the method in Ref. 14 and apply it to the case of periodic crystals. We use the convention that repeated indices are summed. Let us define a unitary transformation

$$\chi_{n\mathbf{R}} = \varphi_{n\mathbf{R}} + \delta\varphi_{n\mathbf{R}} = \varphi_{n'\mathbf{R}'} T_{n'\mathbf{R}',n\mathbf{R}}, \tag{6}$$

$$T_{n'\mathbf{R}',n\mathbf{R}} = \delta_{nn'}\delta_{\mathbf{R}\mathbf{R}'} + \tau_{n'\mathbf{R}',n\mathbf{R}}. \tag{7}$$

From the unitarity of T, one has, to first order,

$$\delta\varphi_{n\mathbf{R}} = \varphi_{n'\mathbf{R}'}\tau_{n'\mathbf{R}',n\mathbf{R}}, \quad \tau^{\dagger}_{n'\mathbf{R}',n\mathbf{R}} + \tau_{n'\mathbf{R}',n\mathbf{R}} = 0. \tag{8}$$

Consider a change in U to first order in $\delta\varphi_{n\mathbf{R}}$:

$$U = \sum_{n\mathbf{R}} \langle \chi^{*}_{n\mathbf{R}}\chi_{n\mathbf{R}}|W|\chi^{*}_{n\mathbf{R}}\chi_{n\mathbf{R}}\rangle, \tag{9}$$

$$\begin{aligned}
\delta U &= \langle \delta\varphi^{*}_{n\mathbf{R}}\varphi_{n\mathbf{R}}|W|\varphi^{*}_{n\mathbf{R}}\varphi_{n\mathbf{R}}\rangle + \langle \varphi^{*}_{n\mathbf{R}}\delta\varphi_{n\mathbf{R}}|W|\varphi^{*}_{n\mathbf{R}}\varphi_{n\mathbf{R}}\rangle \\
&\quad + \langle \varphi^{*}_{n\mathbf{R}}\varphi_{n\mathbf{R}}|W|\delta\varphi^{*}_{n\mathbf{R}}\varphi_{n\mathbf{R}}\rangle + \langle \varphi^{*}_{n\mathbf{R}}\varphi_{n\mathbf{R}}|W|\varphi^{*}_{n\mathbf{R}}\delta\varphi_{n\mathbf{R}}\rangle \\
&= \langle \varphi^{*}_{n'\mathbf{R}'}\varphi_{n\mathbf{R}}|W|\varphi^{*}_{n\mathbf{R}}\varphi_{n\mathbf{R}}\rangle \tau^{*}_{n'\mathbf{R}',n\mathbf{R}} \\
&\quad + \langle \varphi^{*}_{n\mathbf{R}}\varphi_{n'\mathbf{R}'}|W|\varphi^{*}_{n\mathbf{R}}\varphi_{n\mathbf{R}}\rangle \tau_{n'\mathbf{R}',n\mathbf{R}} \\
&\quad + \langle \varphi^{*}_{n\mathbf{R}}\varphi_{n\mathbf{R}}|W|\varphi^{*}_{n'\mathbf{R}'}\varphi_{n\mathbf{R}}\rangle \tau^{*}_{n'\mathbf{R}',n\mathbf{R}} \\
&\quad + \langle \varphi^{*}_{n\mathbf{R}}\varphi_{n\mathbf{R}}|W|\varphi^{*}_{n\mathbf{R}}\varphi_{n'\mathbf{R}'}\rangle \tau_{n'\mathbf{R}',n\mathbf{R}} \\
&= 2\langle \varphi^{*}_{n'\mathbf{R}'}\varphi_{n\mathbf{R}}|W|\varphi^{*}_{n\mathbf{R}}\varphi_{n\mathbf{R}}\rangle \tau^{*}_{n'\mathbf{R}',n\mathbf{R}} \\
&\quad + 2\langle \varphi^{*}_{n\mathbf{R}}\varphi_{n'\mathbf{R}'}|W|\varphi^{*}_{n\mathbf{R}}\varphi_{n\mathbf{R}}\rangle \tau_{n'\mathbf{R}',n\mathbf{R}}.
\end{aligned} \tag{10}$$

This provides an expression for the change of U as a function of parameters $\tau^{*}_{n'\mathbf{R}',n\mathbf{R}}$ and $\tau_{n'\mathbf{R}',n\mathbf{R}}$. Using $\tau^{*}_{n'\mathbf{R}',n\mathbf{R}} + \tau_{n\mathbf{R},n'\mathbf{R}'} = 0$, one can rewrite this expression as follows:

$$\begin{aligned}\delta U &= -2\langle \varphi^*_{n'\mathbf{R}'}\varphi_{n\mathbf{R}}|W|\varphi^*_{n\mathbf{R}}\varphi_{n\mathbf{R}}\rangle\tau_{n\mathbf{R},n'\mathbf{R}'} \\ &\quad + 2\langle \varphi^*_{n\mathbf{R}}\varphi_{n'\mathbf{R}'}|W|\varphi^*_{n\mathbf{R}}\varphi_{n\mathbf{R}}\rangle\tau_{n'\mathbf{R}',n\mathbf{R}} \\ &= 2[\langle \varphi^*_{n\mathbf{R}}\varphi_{n'\mathbf{R}'}|W|\varphi^*_{n\mathbf{R}}\varphi_{n\mathbf{R}}\rangle \\ &\quad - \langle \varphi^*_{n\mathbf{R}}\varphi_{n'\mathbf{R}'}|W|\varphi^*_{n'\mathbf{R}'}\varphi_{n'\mathbf{R}'}\rangle]\tau_{n'\mathbf{R}',n\mathbf{R}} \\ &= 2F^{\dagger}_{n\mathbf{R},n'\mathbf{R}'}\tau_{n'\mathbf{R}',n\mathbf{R}}, \end{aligned} \tag{11}$$

where we have defined an anti-Hermitian matrix ($F^+=-F$)

$$\begin{aligned}F^{\dagger}_{n\mathbf{R},n'\mathbf{R}'} &= \langle \varphi^*_{n\mathbf{R}}\varphi_{n'\mathbf{R}'}|W|\varphi^*_{n\mathbf{R}}\varphi_{n\mathbf{R}}\rangle - \langle \varphi^*_{n\mathbf{R}}\varphi_{n'\mathbf{R}'}|W|\varphi^*_{n'\mathbf{R}'}\varphi_{n'\mathbf{R}'}\rangle \\ &= F^*_{n'\mathbf{R}',n\mathbf{R}}. \end{aligned} \tag{12}$$

We now choose

$$\tau_{n'\mathbf{R}',n\mathbf{R}} = \varepsilon F_{n'\mathbf{R}',n\mathbf{R}}, \tag{13}$$

which ensures that

$$\delta U(\varepsilon) = 2\varepsilon F^{\dagger}_{n\mathbf{R},n'\mathbf{R}'}F_{n'\mathbf{R}',n\mathbf{R}} \geqq 0. \tag{14}$$

The procedure is then the following. Construct the matrix

$$T = e^{\varepsilon F}, \tag{15}$$

which is unitary because F is anti-Hermitian. To calculate T, we diagonalize F with eigenvectors $\langle n\mathbf{R}|\alpha\rangle$ and eigenvalues f_α:

$$T_{n'\mathbf{R}',n\mathbf{R}}(\varepsilon) = \langle n'\mathbf{R}'|\alpha\rangle e^{\varepsilon f_\alpha}\langle\alpha|n\mathbf{R}\rangle. \tag{16}$$

One now obtains a new basis and calculates a new U as a function of ε:

$$\begin{aligned}U(\varepsilon) &= \langle \chi^*_{n\mathbf{R}}\chi_{n\mathbf{R}}|W|\chi^*_{n\mathbf{R}}\chi_{n\mathbf{R}}\rangle \\ &= \langle \varphi^*_{i\mathbf{R}_1}\varphi_{j\mathbf{R}_2}|W|\varphi^*_{k\mathbf{R}_3}\varphi_{l\mathbf{R}_4}\rangle T^*_{i\mathbf{R}_1,n\mathbf{R}}T_{j\mathbf{R}_2,n\mathbf{R}}T^*_{k\mathbf{R}_3,n\mathbf{R}}T_{l\mathbf{R}_4,n\mathbf{R}}. \end{aligned} \tag{17}$$

One varies ε until $U(\varepsilon)$ reaches a maximum and chooses that new basis set $\chi_{n\mathbf{R}}$ that maximizes $U(\varepsilon)$. The procedure is then repeated until convergence is achieved. In practice, we solve for the eigenvectors and eigenvalues of iF, which is Hermitian. The eigenvalues of F are then given by $-i$ times the eigenvalues of iF. The starting orbitals $\varphi_{n\mathbf{R}}$ are chosen to be the maximally localized Wannier orbitals, but other choices are also possible.

The key quantity in the present formulation is the anti-Hermitian matrix F, which is defined with respect to a given cluster. For finite systems such as molecules, it is clear how to apply the above formulation.[14] One simply constructs the matrix F from the definition in Eq. (12), where $\mathbf{R}$ and $\mathbf{R}'$ run over the sites in the molecule. It is not, however, immediately clear how to apply the method to periodic crystals. For this purpose, we define a cluster or supercell around the unit cell (site) at the origin. A new Wannier orbital centered at the origin is constructed as a linear combination of orbitals centered on the sites in the cluster as in Eq. (6). For simplicity but without loss of generality, let us consider the case of one orbital per site (unit cell). First, we note that $F_{\mathbf{R}',\mathbf{R}}$ depends only on the relative distance, $F_{\mathbf{R}',\mathbf{R}}=F_{\mathbf{R}'-\mathbf{R},\mathbf{0}}$. For $\mathbf{R}=\mathbf{0}$, we obtain the first column $F_{\mathbf{R}',\mathbf{0}}$ according to the definition in Eq. (12). We now move to another site $\mathbf{R}$ in the cluster and construct a new Wannier orbital centered on this site $\mathbf{R}$ as a linear combination of orbitals centered on the same cluster sites, but shifted by $\mathbf{R}$ with respect to the cluster centered at the origin. This is to ensure that the Wannier orbitals so constructed will be independent of the sites. The cluster centered at $\mathbf{R}$, however, has some of its sites outside the original cluster centered at the origin. However, there is a correspondence between those sites outside and those sites inside the original cluster: sites connected by superlattice vectors are equivalent. This allows us to construct $F_{\mathbf{R}',\mathbf{R}}$ from $F_{\mathbf{R}',\mathbf{0}}$ in the following way. We search for a superlattice translational vector $\mathbf{T}$ such that

$$\mathbf{R}_0 = \mathbf{R}' - \mathbf{R} - \mathbf{T} \tag{18}$$

is a site in the original cluster centered at the origin. Then the column $F_{\mathbf{R}',\mathbf{R}}$ is given by

$$F_{\mathbf{R}',\mathbf{R}} = F_{\mathbf{R}_0,0}. \tag{19}$$

A given column of F consists of permuted elements of the other columns.

TABLE III. The Hubbard U calculated by maximizing the on-site U compared with the values obtained using the maximally localized Wannier orbitals.

	U_0 (eV)	Max. U (eV)	δU (eV)
Sc	2.444119	2.444175	5.5×10^{-5}
Ti	2.853722	2.853747	2.6×10^{-5}
V	3.216846	3.216978	1.3×10^{-4}
Cr	3.781924	3.782087	1.6×10^{-4}
Mn	3.268736	3.268788	5.2×10^{-5}
Fe	3.619025	3.619095	7.0×10^{-5}
Co	3.097218	3.097302	8.3×10^{-5}
Ni	2.769907	2.769935	2.7×10^{-5}

B. Results

Using the procedure described in the previous section, we have constructed Wannier orbitals by maximizing U for the $3d$ transition metals. The cluster consists of the nearest and next nearest neighbor sites. As can be seen in Table III, the resulting U values are remarkably close to the values calculated using the maximally localized Wannier orbitals. The results do not change in any significant way when only nearest neighbors are included in the cluster. We confirm that the change in U compares favorably with the estimated value in Eq. (14). Indeed, we have checked that the coefficients of expansion $T_{n'\mathbf{R}',n\mathbf{0}}$ are essentially unity when $\mathbf{R}'=\mathbf{0}$ and $n'=n$, and zero otherwise. This implies that the maximally localized Wannier orbitals at the same time, to a very good approximation, maximize the on-site U and form a good basis for the construction of low-energy model Hamiltonians such as the Hubbard model. It is, however, quite feasible that we have not found the global maximum of U. Strictly speak-

TABLE IV. The Hubbard U calculated by maximizing the on-site U (Max. U) for $SrVO_3$. Starting from the maximally localized Wannier orbitals and delocalized orbitals consistently gave the same maximum value of U.

	U_0 (eV)	Max. U (eV)
Localized	3.3808733554	3.3808733554
Delocalized	3.0292927908	3.3808733554

ing, the solution can be a local maximum instead of a global maximum, since the optimization is done by a steepest ascent procedure.

To convince ourselves that our procedure is sound, we have performed the following calculations. We construct a maximally localized Wannier orbital corresponding to the xy orbital of the t_{2g} symmetry of $SrVO_3$ and calculate U. We also construct Wannier orbitals that are deliberately delocalized but span the same Hilbert space as that of the maximally localized ones, and calculate the corresponding U. A $2\times2\times2$ k mesh is used in the calculations. The results are shown in Table IV. As expected, the value of U corresponding to the delocalized orbital is considerably smaller than that corresponding to the maximally localized one. We now construct a Wannier orbital by forming linear combinations of both the maximally localized orbitals and the delocalized ones, and maximize U. The orbitals are centered on sites shown in Table V. The maximum U's calculated from the unitary transformation of the maximally localized orbitals and the delocalized orbitals consistently agree with each other as they should, since the maximally localized orbitals and the delocalized orbitals span the same Hilbert space. As in the case of the $3d$ transition metals, the maximized U is essentially identical to the value corresponding to the maximally localized Wannier orbital. In Table V, we show the distribution of weight, $|T_{\mathbf{R},\mathbf{0}}|^2$, of the orbital that maximizes U formed by a linear combination of the delocalized orbitals. The result indicates that the original maximally localized Wannier orbital centered at (1 1 1) is the only one that has a significant weight at the origin. The corresponding weights for the maximally localized orbitals are almost unity when $\mathbf{R}=\mathbf{0}$, and zero otherwise.

It is remarkable that for the cases considered in the present work, the Wannier orbitals constructed by maximizing the on-site U are almost identical with those of maximally localized Wannier orbitals. Since the screened interaction W_r is deep around the Wannier center, it is reasonable to expect that the maximally localized Wannier orbitals also yield a large value of U close to the maximum value. However, the extreme closeness to the maximum value is rather unexpected. However, as we remarked before, it cannot be excluded that what we have found is a local maximum, not the global maximum of U. We have also performed the same calculations by maximizing the bare Coulomb interaction and found very similar results.

TABLE V. The distribution of weight of the Wannier orbitals that maximize U when starting from delocalized orbitals for $SrVO_3$.

Site	Weight
(0 0 0)	0.939
(0 0 1)	4.1×10^{-8}
(0 1 0)	4.4×10^{-7}
(0 1 1)	4.8×10^{-6}
(1 0 0)	3.1×10^{-7}
(1 0 1)	6.8×10^{-6}
(1 1 0)	6.3×10^{-7}
(1 1 1)	0.061

V. REAL-SPACE APPROACH TO MAXIMALLY LOCALIZED WANNIER ORBITALS

Finally, we propose a real-space approach of constructing maximally localized Wannier orbitals. We construct a unitary transformation on the Wannier orbitals in real space and minimize

$$\Omega = \sum_{\alpha} [\langle r^2 \rangle_{\alpha} - \bar{\mathbf{r}}_{\alpha}^2]. \tag{20}$$

We use a combined notation $\alpha=(\mathbf{R}n)$, and the sum is restricted over the sites in a cluster or supercell. As in the case of maximizing U, consider a small variation

$$\chi_{\alpha} = \varphi_{\alpha} + \delta\varphi_{\alpha}, \tag{21}$$

$$\delta\varphi_{\alpha} = \varphi_{\beta}\tau_{\beta\alpha}, \quad \tau^*_{\alpha\beta} + \tau_{\beta\alpha} = 0, \tag{22}$$

$$\begin{aligned}\Omega &= \sum_{\alpha} [\langle r^2 \rangle_{\alpha} - \bar{\mathbf{r}}_{\alpha}^2] \\ &= \sum_{\alpha} [\langle \chi_{\alpha}|r_{\alpha}^2|\chi_{\alpha}\rangle - \langle \chi_{\alpha}|\mathbf{r}_{\alpha}|\chi_{\alpha}\rangle^2] \\ &= \sum_{\alpha} [\langle \varphi_{\alpha} + \delta\varphi_{\alpha}|r_{\alpha}^2|\varphi_{\alpha} + \delta\varphi_{\alpha}\rangle \\ &\quad - \langle \varphi_{\alpha} + \delta\varphi_{\alpha}|\mathbf{r}_{\alpha}|\varphi_{\alpha} + \delta\varphi_{\alpha}\rangle^2],\end{aligned} \tag{23}$$

$\mathbf{r}_{\alpha}$ means that the position is measured with respect to the origin at site α. The change in Ω to first order in $\delta\varphi$ is

$$\begin{aligned}\delta\Omega &= \sum_{\alpha} [\langle \delta\varphi_{\alpha}|r_{\alpha}^2|\varphi_{\alpha}\rangle + \langle \varphi_{\alpha}|r_{\alpha}^2|\delta\varphi_{a}\rangle \\ &\quad - 2\langle \varphi_{\alpha}|\mathbf{r}_{\alpha}|\varphi_{\alpha}\rangle \cdot \{\langle \delta\varphi_{\alpha}|\mathbf{r}_{\alpha}|\varphi_{\alpha}\rangle + \langle \varphi_{\alpha}|\mathbf{r}_{\alpha}|\delta\varphi_{\alpha}\rangle\}] \\ &= \sum_{\alpha\beta} [\langle \varphi_{\beta}|r_{\alpha}^2|\varphi_{\alpha}\rangle\tau^*_{\beta\alpha} + \langle \varphi_{\alpha}|r_{\alpha}^2|\varphi_{\beta}\rangle\tau_{\beta\alpha} \\ &\quad - 2\langle \varphi_{\alpha}|\mathbf{r}_{\alpha}|\varphi_{\alpha}\rangle \cdot \{\langle \varphi_{\beta}|\mathbf{r}_{\alpha}|\varphi_{\alpha}\rangle\tau^*_{\beta\alpha} + \langle \varphi_{\alpha}|\mathbf{r}_{\alpha}|\varphi_{\beta}\rangle\tau_{\beta\alpha}\}] \\ &= \sum_{\alpha\beta} [\{\langle \varphi_{\alpha}|r_{\alpha}^2|\varphi_{\beta}\rangle - 2\langle \varphi_{\alpha}|\mathbf{r}_{\alpha}|\varphi_{\alpha}\rangle \cdot \langle \varphi_{\alpha}|\mathbf{r}_{\alpha}|\varphi_{\beta}\rangle\}\tau_{\beta\alpha} \\ &\quad - \{\langle \varphi_{\alpha}|r_{\beta}^2|\varphi_{\beta}\rangle - 2\langle \varphi_{\beta}|\mathbf{r}_{\beta}|\varphi_{\beta}\rangle \cdot \langle \varphi_{\alpha}|\mathbf{r}_{\beta}|\varphi_{\beta}\rangle\}\tau_{\beta\alpha}] \\ &= \sum_{\alpha\beta} [\langle \varphi_{\alpha}|r_{\alpha}^2|\varphi_{\beta}\rangle - \langle \varphi_{\alpha}|r_{\beta}^2|\varphi_{\beta}\rangle]\tau_{\beta\alpha} \\ &\quad + 2[\langle \varphi_{\beta}|\mathbf{r}_{\beta}|\varphi_{\beta}\rangle \cdot \langle \varphi_{\alpha}|\mathbf{r}_{\beta}|\varphi_{\beta}\rangle \\ &\quad - \langle \varphi_{\alpha}|\mathbf{r}_{\alpha}|\varphi_{\alpha}\rangle \cdot \langle \varphi_{\alpha}|\mathbf{r}_{\alpha}|\varphi_{\beta}\rangle]\tau_{\beta\alpha}.\end{aligned} \tag{24}$$

As in the case of maximizing U, we define an anti-Hermitian matrix

$$F_{\alpha\beta} = \langle\varphi_\alpha|r_\alpha^2|\varphi_\beta\rangle - \langle\varphi_\alpha|r_\beta^2|\varphi_\beta\rangle + 2[\langle\varphi_\beta|\mathbf{r}_\beta|\varphi_\beta\rangle \cdot \langle\varphi_\alpha|\mathbf{r}_\beta|\varphi_\beta\rangle - \langle\varphi_\alpha|\mathbf{r}_\alpha|\varphi_\alpha\rangle \cdot \langle\varphi_\alpha|\mathbf{r}_\alpha|\varphi_\beta\rangle], \quad (25)$$

and choose for the steepest descent method

$$\tau = -\varepsilon F^\dagger. \quad (26)$$

The rest of the procedure is identical to the case of maximizing U. We can write $\mathbf{r}_\alpha = \mathbf{R}_\beta - \mathbf{R}_\alpha + \mathbf{r}_\beta$, implying that $\langle\varphi_\alpha|\mathbf{r}_\alpha|\varphi_\beta\rangle = \langle\varphi_\alpha|\mathbf{r}_\beta|\varphi_\beta\rangle$. For a one-band case, it follows that the third and fourth terms in $F_{\alpha\beta}$ vanish. The applicability of this scheme depends crucially on the feasibility of computing the quantities $\langle\varphi_\alpha|r_\alpha^2|\varphi_\beta\rangle$ and $\langle\varphi_\alpha|\mathbf{r}_\alpha|\varphi_\beta\rangle$. Once these quantities are available, the minimization process is relatively simple.

Following Ref. 5, the spread functional can be split according to

$$\Omega = \Omega_I + \tilde{\Omega}, \quad (27)$$

$$\Omega_I = \sum_\alpha \left[\langle r^2\rangle_\alpha - \sum_\beta |\langle\varphi_\beta|\mathbf{r}_\alpha|\varphi_\alpha\rangle|^2 \right], \quad (28)$$

$$\tilde{\Omega} = \sum_\alpha \sum_{\beta\neq\alpha} |\langle\varphi_\beta|\mathbf{r}_\alpha|\varphi_\alpha\rangle|^2. \quad (29)$$

The quantity Ω_I is independent of the unitary transformation. We could equally apply the minimization procedure to $\tilde{\Omega}$, instead of Ω.

VI. CONCLUDING REMARKS

We have shown the usefulness of the maximally localized Wannier function as a basis for the downfolding procedure. It is found that in transition metals, the values of the screened Coulomb interaction are in reasonable agreement with those from previous calculations based on the LMTO-ASA. The somewhat smaller values of the present calculations may be attributed to the more extended nature of the Wannier orbitals compared with the more localized truncated partial waves used in taking the matrix elements of the screened interaction in the previous calculations. Unexpectedly, we have found that for the cases we have considered, the maximally localized Wannier functions are remarkably close to the Wannier function that maximizes the on-site Coulomb interaction. Although we have no proof, it is quite likely that this property persists in many other systems. This makes the maximally localized Wannier orbitals a very suitable basis for constructing low-energy model Hamiltonians.

We have also proposed a real-space approach for constructing maximally localized Wannier orbitals, which may be another practical procedure other than the k-space approach. The applicability of this scheme, however, remains to be seen.

There have been many attempts for combining first-principles methods with many-body techniques (DMFT and its extensions, path integral renormalization group method,[42] etc.). The present technique would be useful for the application of these methods to real materials. In particular, we have in mind the recently developed GW+DMFT scheme, to which the present maximally localized Wannier orbitals are now being applied.

ACKNOWLEDGMENTS

We thank T. Kotani, M. Imada, K. Nakamura, R. Arita, and S. Biermann for fruitful discussions. This work was supported by Grant-in-Aid for Scientific Research from MEXT Japan (Grants No. 19019013 and No. 19051016). We also acknowledge computer facility from the supercomputer center at ISSP, University of Tokyo.

[1] O. Gunnarsson, O. K. Andersen, O. Jepsen, and J. Zaanen, Phys. Rev. B **39**, 1708 (1989).
[2] O. Gunnarsson, Phys. Rev. B **41**, 514 (1990).
[3] F. Aryasetiawan, M. Imada, A. Georges, G. Kotliar, S. Biermann, and A. I. Lichtenstein, Phys. Rev. B **70**, 195104 (2004).
[4] I. V. Solovyev, Phys. Rev. B **73**, 155117 (2006).
[5] N. Marzari and D. Vanderbilt, Phys. Rev. B **56**, 12847 (1997).
[6] I. Souza, N. Marzari, and D. Vanderbilt, Phys. Rev. B **65**, 035109 (2001).
[7] O. K. Andersen and T. Saha-Dasgupta, Phys. Rev. B **62**, R16219 (2000); Bull. Mater. Sci. **26**, 19 (2003).
[8] F. Lechermann, A. Georges, A. Poteryaev, S. Biermann, M. Posternak, A. Yamasaki, and O. K. Andersen, Phys. Rev. B **74**, 125120 (2006).
[9] R. D. King-Smith and D. Vanderbilt, Phys. Rev. B **47**, 1651 (1993).
[10] F. Giustino, Jonathan R. Yates, I. Souza, M. L. Cohen, and G. Louie, Phys. Rev. Lett. **98**, 047005 (2007).
[11] X. Wang, J. R. Yates, I. Souza, and D. Vanderbilt, Phys. Rev. B **74**, 195118 (2006).
[12] J. R. Yates, X. Wang, D. Vanderbilt, and I. Souza, Phys. Rev. B **75**, 195121 (2007).
[13] T. Miyake, P. Zhang, M. L. Cohen, and S. G. Louie (unpublished).
[14] C. E. Edmiston and K. Ruedenberg, Rev. Mod. Phys. **35**, 457 (1963).
[15] S. F. Boys, in *Quantum Theory of Atoms, Molecules, and the Solid State*, edited by P.-O. Löwdin (Academic, New York, 1966).
[16] V. I. Anisimov, J. Zaanen, and O. K. Andersen, Phys. Rev. B **44**, 943 (1991).
[17] K. Nakamura, R. Arita, Y. Yoshimoto, and S. Tsuneyuki, Phys. Rev. B **74**, 235113 (2006).
[18] F. Aryasetiawan, K. Karlsson, O. Jepsen, and U. Schonberger, Phys. Rev. B **74**, 125106 (2006).
[19] M. Springer and F. Aryasetiawan, Phys. Rev. B **57**, 4364 (1998).

[20] T. Kotani, J. Phys.: Condens. Matter **12**, 2413 (2000).
[21] I. V. Solovyev and M. Imada, Phys. Rev. B **71**, 045103 (2005).
[22] M. Cococcioni and S. de Gironcoli, Phys. Rev. B **71**, 035105 (2005).
[23] W. Kohn and L. J. Sham, Phys. Rev. **140**, A1133 (1965).
[24] P. Hohenberg and W. Kohn, Phys. Rev. **136**, B864 (1964).
[25] V. I. Anisimov, F. Aryasetiawan, and A. I. Lichtenstein, J. Phys.: Condens. Matter **9**, 767 (1997).
[26] For reviews, see *Strong Coulomb correlations in Electronic Structure Calculations*, edited by V. I. Anisimov, Advances in Condensed Material Science (Gordon and Breach, New York, 2001).
[27] A. Georges and G. Kotliar, Phys. Rev. B **45**, 6479 (1992).
[28] A. Georges, G. Kotliar, W. Krauth, and M. J. Rosenberg, Rev. Mod. Phys. **68**, 13 (1996).
[29] V. I. Anisimov, A. I. Poteryaev, M. A. Korotin, A. O. Anokhin, and G. Kotliar, J. Phys.: Condens. Matter **9**, 7359 (1997).
[30] P. Sun and G. Kotliar, Phys. Rev. B **66**, 085120 (2002).
[31] S. Biermann, F. Aryasetiawan, and A. Georges, Phys. Rev. Lett. **90**, 086402 (2003).
[32] I. Paul and G. Kotliar, Eur. Phys. J. B **51**, 189 (2006).
[33] O. K. Andersen, Phys. Rev. B **12**, 3060 (1975).
[34] W. Ku, H. Rosner, W. E. Pickett, and R. T. Scalettar, Phys. Rev. Lett. **89**, 167204 (2002).
[35] M. Methfessel, M. van Schilfgaarde, and R. A. Casali, *Lecture Notes in Physics*, edited by H. Dreysse (Springer-Verlag, Berlin, 2000), Vol. 535.
[36] T. Miyake and F. Aryasetiawan, Phys. Rev. B **61**, 7172 (2000).
[37] F. Aryasetiawan and O. Gunnarsson, Phys. Rev. B **49**, 16214 (1994).
[38] F. Aryasetiawan, in *Strong Coulomb Correlations in Electronic Structure Calculations*, edited by V. I. Anisimov (Gordon and Breach, Singapore, 2000).
[39] T. Kotani and M. van Schilfgaarde, Solid State Commun. **121**, 461 (2002).
[40] M. van Schilfgaarde, T. Kotani, and S. V. Faleev, Phys. Rev. B **74**, 245125 (2006).
[41] T. Kotani, M. van Schilfgaarde, and S. V. Faleev, Phys. Rev. B **76**, 165106 (2007).
[42] M. Imada and T. Kashima, J. Phys. Soc. Jpn. **69**, 2723 (2000); T. Kashima and M. Imada, *ibid.* **70**, 2287 (2001).